JACS
JOURNAL OF THE AMERICAN CHEMICAL SOCIETY

ARTICLE

pubs.acs.org/JACS

Amphiphilic Crescent-Moon-Shaped Microparticles Formed by Selective Adsorption of Colloids

Shin-Hyun Kim, Alireza Abbaspourrad, and David A. Weitz*

School of Engineering and Applied Sciences and Department of Physics, Harvard University, Cambridge, Massachusetts, United States

Supporting Information Web-Enhanced

ABSTRACT: We use a microfluidic device to prepare monodisperse amphiphilic particles in the shape of a crescent-moon and use these particles to stabilize oil droplets in water. The microfluidic device is comprised of a tapered capillary in a theta (θ) shape that injects two oil phases into water in a single receiving capillary. One oil is a fluorocarbon, while the second is a photocurable monomer, which partially wets the first oil drop; silica colloids in the monomer migrate and adsorb to the interface with water but do not protrude into the oil interface. Upon UV-induced polymerization, solid particles with the shape of a crescent moon are formed; removal of fluorocarbon oil yields amphiphilic particles due to the selective adsorption of silica colloids. The resultant amphiphilic microparticles can be used to stabilize oil drops in a mixture of water and ethanol; if they are packed to sufficient surface density on the interface of the oil drop, they become immobilized, preventing direct contact between neighboring drops, thereby providing the stability.

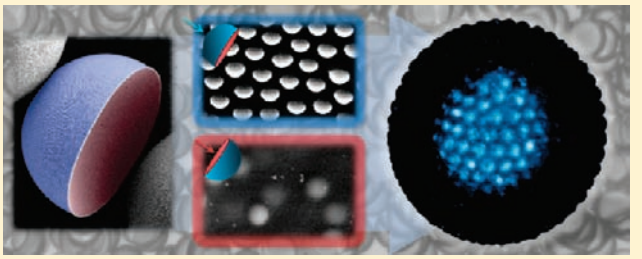

INTRODUCTION

Anisotropic microparticles have great potential as a new class of colloidal materials with advanced functionalities.[1,2] For example, Janus particles can be used as active pigments in new types of display devices,[3,4] while chemically patterned microparticles can be used as building blocks to construct photonic structures through directional interactions.[5,6] Of particular interest is in amphiphilic microparticles, which are useful for stabilization of the interface between two immiscible fluids.[7] Amphiphilic Janus microparticles have been prepared by selective surface modification of spherical microparticles through masking techniques, directional deposition, and stamping.[8−11] Even further enhancement of the stability and controllability of interface shape can be achieved with amphiphilic microparticles with anisotropic shape. However, there exist few methods to produce microparticles that are anisotropic in both their properties and their shape. Polymerization of cross-linked spherical particle templates swollen with monomers can yield dumbbell-like amphiphilic microparticles which can be used as colloidal surfactants for stabilization of oil drops in water.[12,13] Alternatively, wedge-shaped amphiphilic microparticles can be prepared by a continuous flow lithography technique,[14] and mushroom-shaped microparticles of tunable amphiphilic property can be prepared by phase separation of two different polymers confined in emulsion droplets.[15] However, by analogy to molecular surfactants, which cover a full spectrum of hydrophilic−lipophilic balance, shape, size, and contrast of hydrophobicity and hydrophilicity, so too should amphiphilic microparticles exhibit wide diversity. Thus, there still remains intense demand for new classes of microparticles that are both amphiphilic and anisotropic in shape that can be used to stabilize fluid−fluid interfaces.

In this paper, we report a facile and pragmatic approach to make monodisperse amphiphilic microparticles that are highly anisotropic, with a crescent-moon shape, consisting of hydrophilic convex and hydrophobic concave surfaces. With a capillary microfluidic device, monodisperse paired oil droplets of fluorocarbon and photocurable monomer are prepared in water. The monomer droplets contain silica particles, which spontaneously adsorb at the aqueous interface but do not adsorb at the fluorocarbon−oil interface. After polymerization of monomer droplets and subsequent removal of fluorocarbon droplets, two different surfaces remain on each microparticle, resulting in crescent-moon-shaped amphiphilic microparticles, which can be used to stabilize oil drops in water. Unlike molecular surfactants, which lower interfacial tension, these amphiphilic particles are densely packed at the oil−water interface, thereby preventing direct contact between neighboring drops because they are immobilized.

RESULTS AND DISCUSSION

Paired Droplets and Core−Shell Droplets. To emulsify two immiscible oil phases together in an aqueous phase, we employ microfluidic devices constructed from a capillary in a theta (θ) shape that is tapered to a narrow aperture. This cylindrical capillary is inserted in a second square capillary whose inner dimension is the same as that of outer diameter of cylindrical capillary; this is shown schematically in Figure 1a. We flow

Received: January 6, 2011
Published: March 21, 2011

dx.doi.org/10.1021/ja200139w | J. Am. Chem. Soc. 2011, 133, 5516–5524

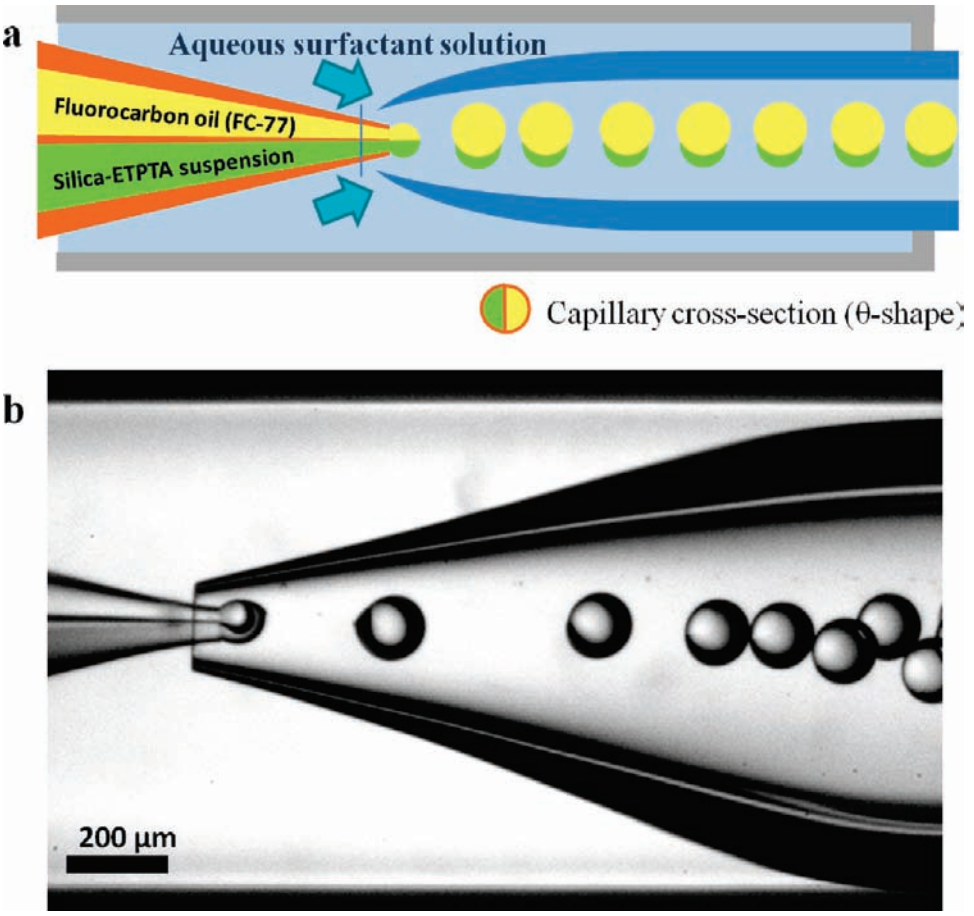

Figure 1. (a) Schematic illustration of the microfluidic device comprised of a tapered theta (θ)-shaped capillary for injection of two immiscible oil phases and a circular capillary for droplet collection. (b) Optical microscope image showing droplet generation in a dripping mode.

monomer of ethoxylated trimethylolpropane triacrylate (ETPTA) through one side of the cylindrical capillary and fluorocarbon oil (FC-77) through the second side. We flow an aqueous surfactant solution through the square capillary to form the continuous phase. To increase the velocity of the continuous phase near the tip of the injection capillary, we insert a second circular capillary to confine the flow near the injection tip, thereby increasing the flow velocity. When operating in the dripping mode, each drop consists of two distinct components as shown in Figure 1b; here, the upper phase is FC-77 while the lower phase is ETPTA. Upon formation of the drop, the ETPTA immediately spreads on the surface of the FC-77 droplet to reduce the interfacial area of high surface tension between FC-77 and water. The final shape of the drop depends on the surfactant in the aqueous phase, which controls the spreading parameter, S. For 1 wt % of ethylene oxide−propylene oxide−ethylene oxide triblock copolymer (Pluronic F-108), ETPTA dewets on the surface of FC-77 and forms a second distinct droplet as shown in Figures 2a,b and Movie S1; here, the small dark portion of the drop is ETPTA. By contrast, for 3 wt % poly(vinyl alcohol) (PVA), the ETPTA completely wets the surface of FC-77, resulting in a core−shell droplet as shown in Figures 2c,d and Movie S1. The behavior is determined by the relative surface energies of the three fluids and can be summarized by the behavior of spreading parameter,

$$S_i = \gamma_{jk} - (\gamma_{ij} + \gamma_{ik}) \quad (1)$$

where γ_{jk} is interfacial tension between phase j and k.[16−18] The spreading parameter reflects the relative values of the surface energies, and the propensity of one fluid to spread on a second. The surface tensions of the two oils with water are very high, so the spreading parameter of water on each oil, S_w, is strongly negative. As a result, the two oil drops never separate, but always remain paired. However, the spreading of the ETPTA on the FC-77 depends on the values of the spreading parameter and can be controlled through the addition of surfactant. In all cases, the surface energy of water with FC-77 is greater than that of ETPTA, $\gamma_{F,w} > \gamma_{E,w}$. Thus the ETPTA will completely spread over the surface, forming a core−shell structure if $S_E > 0$, but will remain a separate drop if $S_E < 0$.[19,20] We measure the surface tension of the FC-77 with ETPTA to be $\gamma_{F,E} = 13.59$ mN/m. For the surfactant F-108, we measure $\gamma_{F,w} = 16.97$ mN/m; however, we are unable to obtain a reliable measurement for $\gamma_{E,w}$, and instead estimate it to be $\gamma_{E,w} \approx 5$ mN/m from simulations of the shape of the drops using *surface evolver*.[21] Thus, $S_E \approx -1.62$ mN/m and is negative, so the drops remain separate, forming a paired drop, as shown in Figure 2a,b. By contrast, when PVA is used as a surfactant, $\gamma_{F,w} = 20.26$ mN/m, while $\gamma_{E,w} = 2.24$ mN/m, $S_E \approx 4.43$ mN/m and is positive, so the ETPTA spreads completely, forming a core−shell structure, as shown in Figure 2c,d. By photopolymerization of the shell, solid core−shell structures can be prepared, as shown in Figure 2e,f.

Amphiphilic Microparticles. To prepare amphiphilic microparticles, we use the paired droplets stabilized with F-108 and follow the strategy illustrated schematically in Figure 3a. The ETPTA

dx.doi.org/10.1021/ja200139w | *J. Am. Chem. Soc.* 2011, 133, 5516–5524

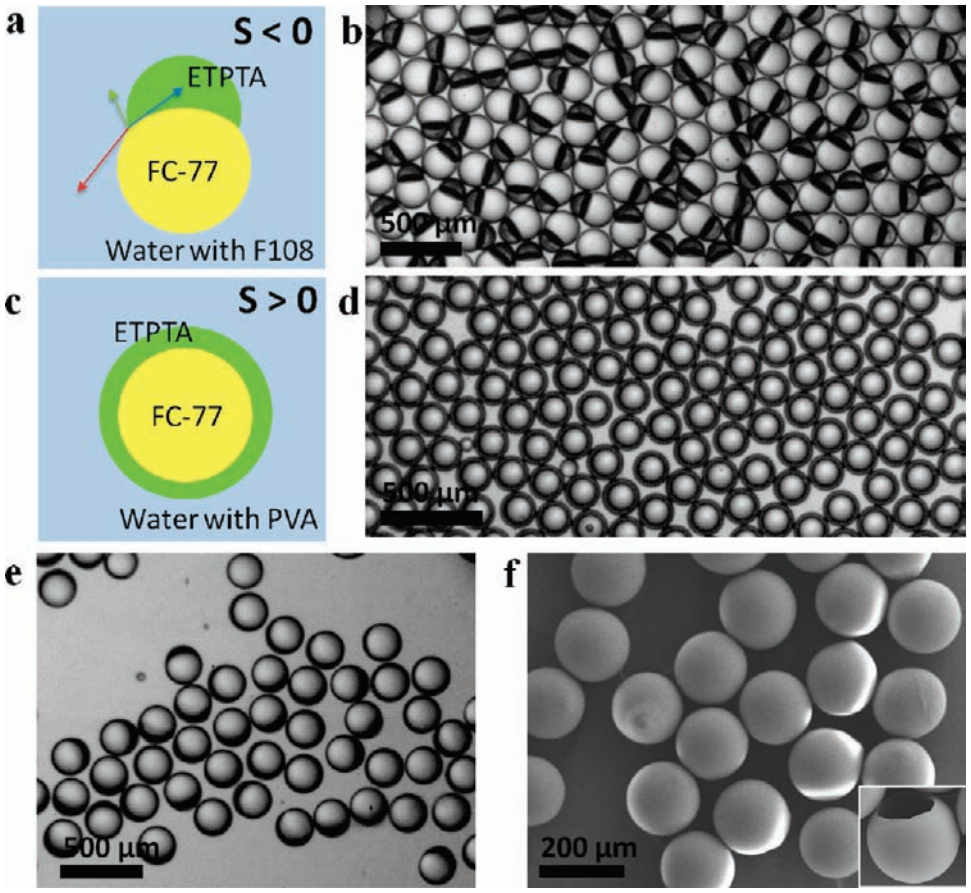

Figure 2. (a) Formation of paired oil droplet for a negative spreading parameter of ETPTA. (b) Optical microscope image of monodisperse paired droplets of fluorocarbon oil and monomer. (c) Formation of core−shell droplet for a positive spreading parameter of ETPTA. (d) Optical microscope image of core−shell droplets of fluorocarbon core and monomer shell. (e,f) Optical microscope and SEM images of microcapsules prepared by polymerization of shell phase of core−shell droplets. Inset of panel f shows hollow core of crushed capsule.

droplets contain bare hydrophilic silica particles which spontaneously migrate and adsorb to the interface with water, where they minimize the total interfacial energy by reducing the interfacial area between ETPTA and water.[22,23] However, the particles do not protrude into the interface with FC-77 because of the high energy cost for hydrophilic silica particles to contact the FC-77. The reduction of the energy per silica particle when anchored at the water−ETPTA interface is much larger than thermal energy, and therefore, once trapped, the particles cannot escape the interface. We photopolymerize the monomer drops and then disperse the drop pairs in ethanol to induce coalescence of FC-77 oil drops, enabling the FC-77 to be removed. This leaves crescent-moon-shaped microparticles with two different surfaces: a convex surface with exposed silica particles and a concave surface with no exposed silica particles. The optical microscope images of polymerized paired droplets and resultant monodisperse microparticles in the mixture of water and ethanol in a volume ratio of 1:1 are shown in Figure 3, panels b,c and d,e, respectively; here, the volumetric flow rates of ETPTA and FC-77 in the microfluidic device are in a ratio of 1:4. The microparticles sediment and stack by overlapping their convex surfaces with the concave surfaces of neighboring particles, as shown in Figure 3e. The microparticles are optically transparent because of the small refractive-index mismatch between silica (n_{silica} = 1.45) and ETPTA (n_{ETPTA} = 1.4689).

The selective adsorption of silica particles is confirmed by SEM analysis. Moiré fringes appear on the convex surfaces of the microparticles, which are covered by the silica nanoparticles, but fringes do not appear on the concave surfaces at the specific SEM magnification used in Figure 4a. The moiré fringes are caused by the interaction between two overlapping, regular patterns. The hexagonal arrays of silica particles produce this fringe when interacting with the scanning line pattern of the SEM.[24] Therefore, the observation of fringes on only the convex surface is pronounced evidence of selective adsorption of silica particles on these surfaces. At high magnification, we observe the hexagonal arrays of protruding silica particles, 380 nm in diameter, on the convex surface as shown in Figure 4b,c. The contact angle of silica particles from the ETPTA side can be calculated to be 70° through simple geometric considerations. The concave surfaces of the microparticles do not have exposed silica particles as shown in Figure 4d,e. Although the surface undulates irregularly, the particles are fully embedded in ETPTA matrix as seen in Figure 4e.

To evaluate the difference in the surface properties between ETPTA with and without exposed silica particles, we prepare two sets of spherical microparticles from monodisperse single emulsion droplets, the first consisting of a silica−ETPTA suspension and the second consisting of a particle-free ETPTA monomer. The microparticles with the smooth ETPTA surface show a contact angle of 36.7° when they are anchored at the interface between air and water as shown in Figure S1a of Supporting Information. By contrast, the microparticles formed from the

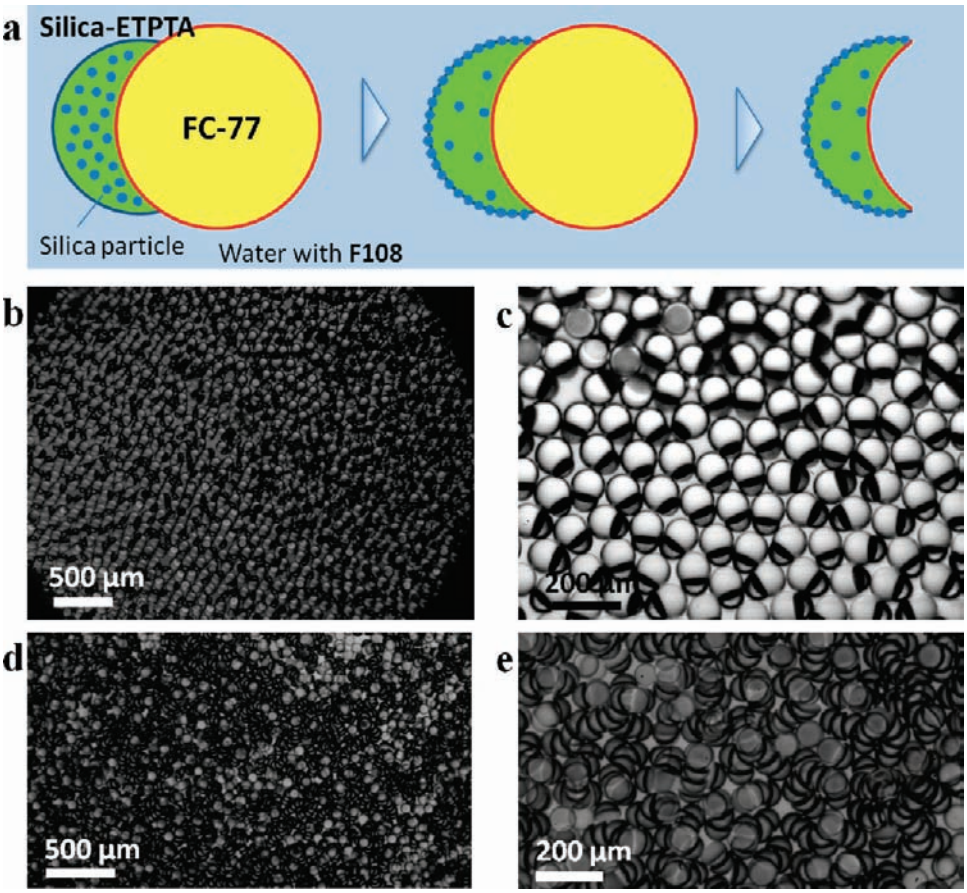

Figure 3. (a) Schematic illustration of the method to make an amphiphilic microparticle from a paired droplet. Silica particles in the monomer droplet adsorb selectively to the interface with water, but do not adsorb to the interface with fluorocarbon oil. (b, c) Optical microscope images of polymerized paired drops. (d, e) Amphiphilic microparticles prepared by removal of fluorocarbon oil drops.

silica−ETPTA suspension, which have hexagonal arrays of silica particles over the whole surface, show a contact angle of 8.4°. Thus, the dense arrays of hydrophilic silica nanodomes on the ETPTA surface significantly increase the hydrophilicity of the microparticle. We conclude, therefore, that the convex surfaces of the crescent-moon microparticles are relatively more hydrophilic whereas the concave surfaces are relatively more hydrophobic.

The size and shape of the microparticles themselves can be controlled by the relative volumetric flow rates of ETPTA (V_1) and FC-77 (V_2); as the ratio is increased, the relative size of the ETPTA lobe increases, as summarized in Figure 5. The first row in Figure 5 shows a simulation of the shapes of the drop pairs using *surface evolver*, where the total surface energy is minimized for each volume ratio, and the surface energies are set to $\gamma_{F,w} = 16.97$ mN/m and $\gamma_{F,E} = 13.59$ mN/m and where we match the simulated shapes to those obtained experimentally, shown in the second row, by using $\gamma_{E,w} = 5$ mN/m. We determine the shapes of the resultant microparticles, obtained by photopolymerizing the ETPTA and removing the FC-77, using *surface evolver*, and display them in the third row; these are in good accord with the shapes determined from SEM images of the microparticles, shown in the fourth row. Optical microscope and SEM images of monodisperse microparticles with different volume ratios at low magnification are displayed in Figure S2 of Supporting Information.

Stabilization of Oil Drops with Amphiphilic Microparticles. The crescent-moon-shaped amphiphilic microparticles provide a new shape that can significantly enhance the stability of interfaces of oil and water and can provide added controllability of interfacial shapes by comparison to spherically shaped amphiphilic microparticles. In particular, crescent-moon-shaped microparticles have structural advantages in the stabilization of emulsion drops compared with spherical particles with similar size and compared with other nonspherical amphiphilic microparticles.[8−15,25] First, unlike spherically shaped microparticles, the body of the crescent-moon-shaped microparticle does not enter into the dispersed phase of the emulsion; instead, a contact line is formed along the outermost edge of the crescent-moon. This maximizes the fraction of interface that is protected by obviating body hindrance and therefore provides higher stability. In addition, relatively small volumes of emulsion drops can also be stabilized with negligible increase of unprotected interface area by the folding of densely packed microparticles.

To illustrate these effects, we stabilize oil drops in a mixture of water and ethanol with a volume ratio of 1:1 using amphiphilic microparticles with $V_1/V_2 = 0.25$, which have a diameter of 75 μm and a thickness of 27 μm. When the microparticle suspensions are shaken with a small volume of FC-77 oil, the microparticles adsorb at the interface of the oil drops and align themselves so that the hydrophobic concave surfaces always

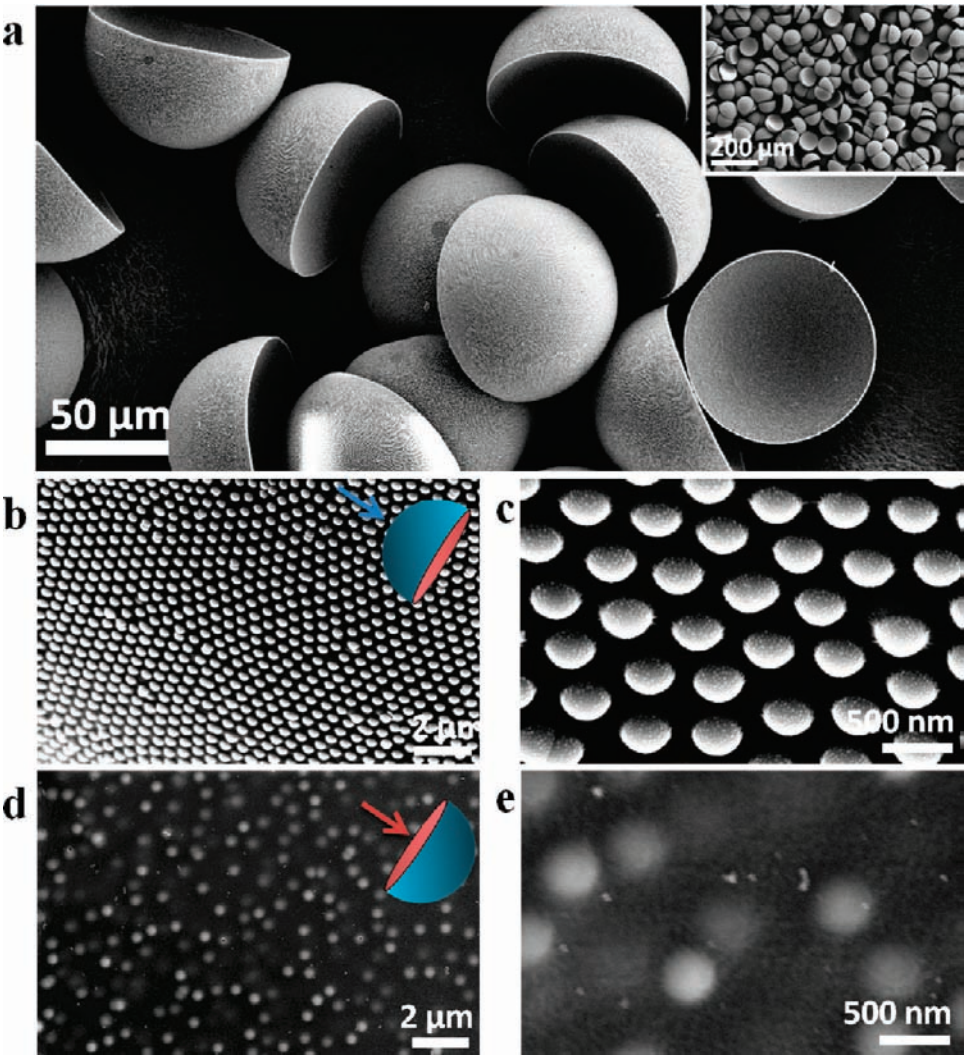

Figure 4. (a) SEM image of amphiphilic microparticles, which show moiré fringe only on convex surfaces. Inset is an SEM image of low magnification. (b, c) SEM images of convex surface at high magnification showing hexagonal arrays of exposed silica particles. (d, e) Concave surface of microparticles which do not have exposed silica particles. SEM image of panel e reveals that all silica particles are buried in polymer matrix.

contact the oil while the hydrophilic convex surfaces always face the continuous phase, as shown in Figure 6a. Even a very small volume oil drop can be covered by just a few microparticles; even a pair of two particles can completely cover the whole interface of a small enough oil drop by facing each other, as shown in Figure 6b where the volume of the oil drop is just 47.6 pL, approximately half the volume of one microparticle (86.7 pL), which is calculated from geometric considerations. This prevents coalescence of the oil drops even with significant mechanical collisions between neighboring pairs. When the oil volume is too small to fully occupy the space confined by two or three concave surfaces, the microparticles shift their positions to engulf the oil drop, as denoted with dotted ellipses for two microparticles and with dotted circles for three microparticles in Figure 6b. These fan-shaped configurations of three microparticles are frequently observed during oil stabilization. In the absence of oil, the microparticles pack by overlapping their convex surfaces with concave surfaces of neighboring particles, as seen in Figure 3e. Optical microscope images of a stabilized oil drop with many microparticles taken at three different focal planes, in the top, middle, and bottom of the drop show that whole interface of the drop is covered by aligned microparticle arrays, as seen in Figure 6c.

We stabilize different types of oil drops such as silicone oil and hexadecane with amphiphilic microparticles. Coated silicone oil drops are displayed in Figure 6d and Figure S3 of Supporting Information. Interestingly, nonspherical coated drops are frequently observed; this is presumably due to the immobilization of the interface by a close-packed array of the microparticles.[26] The stability of coated drops is evaluated using a square capillary that is equipped with two circular rods; here, one rod is fixed and the other one is movable. When two coated silicone oil drops are confined in the square capillary, between the two circular rods, the drops remain stable, even when they contact one another (1.7 s) and are squeezed together (4.1 s) as the movable rod pushes against the drops, as shown in Figure 7 and Movie S2 where the contact line of microparticles on the interface is clearly shown. When the movable rod is retracted (11.1 s), the original drops are recovered; thus, direct contact between the inner fluid interfaces is prevented by the anchored arrays of microparticles. By contrast, surfactant does not afford the same stability to the

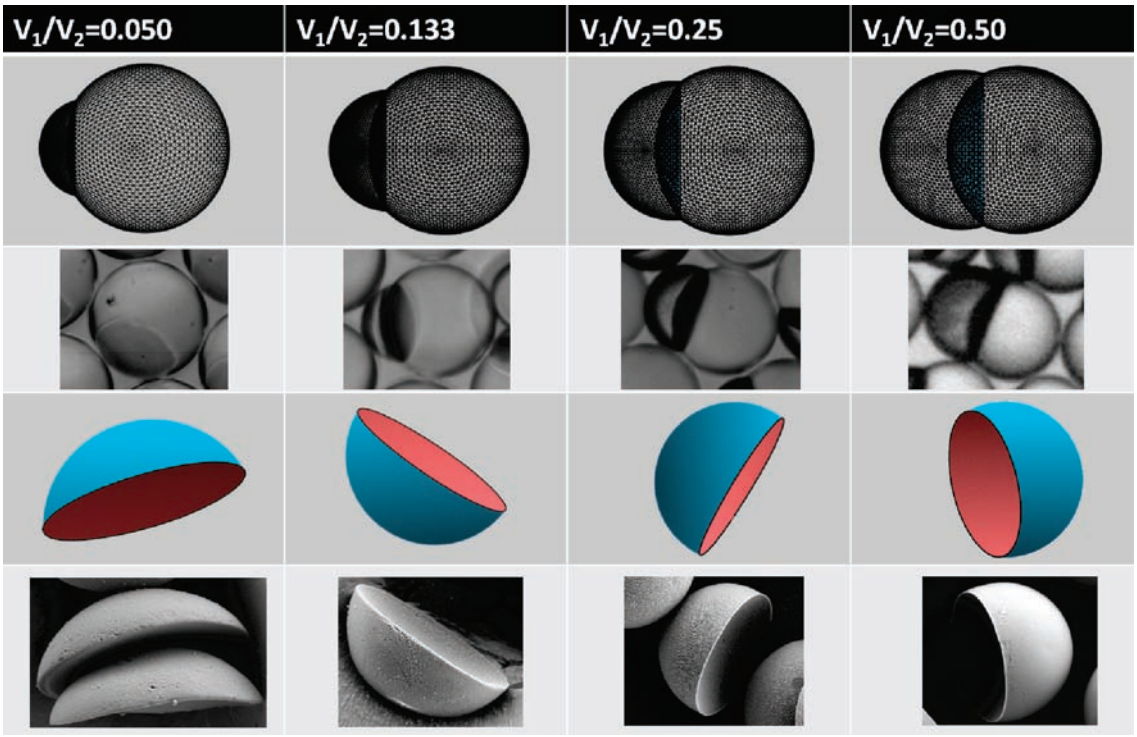

Figure 5. The control of particle size and shape according to relative volumetric flow rates of monomer (V_1) and fluorocarbon oil (V_2). First and second rows show *surface evolver* simulation and optical microscope images of paired droplets, whereas third and fourth rows show *surface evolver* and SEM images of resultant microparticles.

drops, and they readily coalesce when they are squeezed together. Movie S3 demonstrates the clear difference between surfactant-stabilized interface and microparticle-coated interfaces; for the comparison, we employ silicone oil drops stabilized by PVA, which does not prevent direct contact with the rounded end of a glass cone.

The microparticles can pack densely on the interfaces; this immobilizes the interfaces, allowing them to sustain unequal stresses, enabling them to sustain nonspherical shapes.[26] For example, a silicone oil drop maintains a nonspherical shape due to the anchored microparticles as shown in the first image in Figure 8a. When we squeeze this drop in the square capillary using the movable rod (2.4 s), the drop adopts a new shape by fitting its body into the confining geometry. The drop retains its shape, leaving a square-disk shape after removal of the rod (4.1 s). When we poke the densely packed interface of the silicone oil drop using a glass cone with a rounded end, the interface is indented by the contact with the cone but is not punctured (1.1 s), as shown in Figure 8b. The interface maintains the dent even after the cone is removed, although the depth of the indentation is reduced as the interface relaxes (1.4 s). The immobilization of the interface is displayed explicitly in the second part of Movie S2.

Dissolution of the inner drop fluid into the continuous phase reduces the volume and thus deforms the drop shape. Because the surface area of the interface is maintained by the close-packed monolayer of microparticles, the drop must deform from a spherical shape. Thus, spherical silicone oil drops evolve into nonspherical ones over the course of 15 days due to the slow dissolution of silicone oil into the continuous water−ethanol phase. Optical microscope images of a deformed drop, taken at three different focal planes, exhibit the faceted structure, as shown in Figure S4 in Supporting Information. The faces are composed of hexagonal arrays of microparticles while the 5-fold symmetric microparticles, which are inevitably found on a closed surface,[27] form the vertices of the structure. This observation is in accord with a previous report on dissolution of air bubbles coated with particles.[28]

The shape of the microparticles can make differences in stabilization of oil drops. The microparticles with low curvatures (first column in Figure 5) are appropriate for stabilization of large oil drops because of low deformation of the oil−water interface. By contrast, the microparticles with high curvature (last column in Figure 5) cannot form close-packed circles of contact line on the interface of a large oil drop due to the hindrance by the larger diameter of the convex surface compared with the edge diameter. However, the high curvatures have an advantage for stabilization of a small oil drop because the wider space between concave surfaces of a pair or a few microparticles can hold a larger volume of oil.

Enhancement of Microparticle Functionality. The contrast of the wetting properties between the convex and concave surfaces can be further enhanced by using a mixture of silica particles in the ETPTA, with both the bare hydrophilic silica particles and octadecyltrimethoxysilane (OTMOS)-treated silica particles, which are hydrophobic. The particles each adsorb at different interfaces; the bare silica particles adsorb to the water interface while the OTMOS-treated silica particles adsorb to the FC-77 interface, as illustrated schematically in Figure 9a. The resultant microparticles have an enhanced contrast between the hydrophilic and hydrophobic interfaces. SEM images of amphiphilic microparticles produced from a suspension of 186-nm-diameter bare silica particles and 1-μm-diameter OTMOS-treated silica particles are shown in

dx.doi.org/10.1021/ja200139w |*J. Am. Chem. Soc.* 2011, 133, 5516–5524

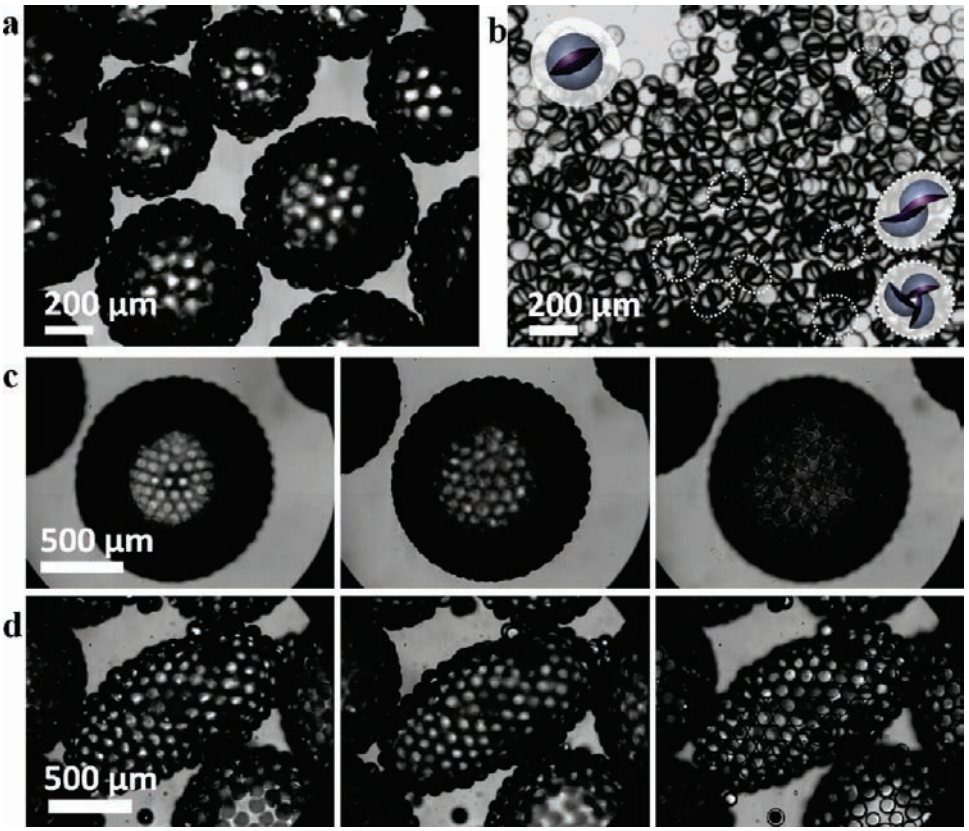

Figure 6. (a−c) Optical microscope images of fluorocarbon oil drops stabilized by amphiphilic microparticles. A small-volume oil droplet can be covered by a pair of microparticles or a few microparticles as shown in panel b. The three images in panel c, taken at three different focal planes in the top, middle, and bottom of the drop, show that the whole interface of drop is covered by microparticles. (d) Images of a nonspherical coated silicone oil drop taken at three different focal planes.

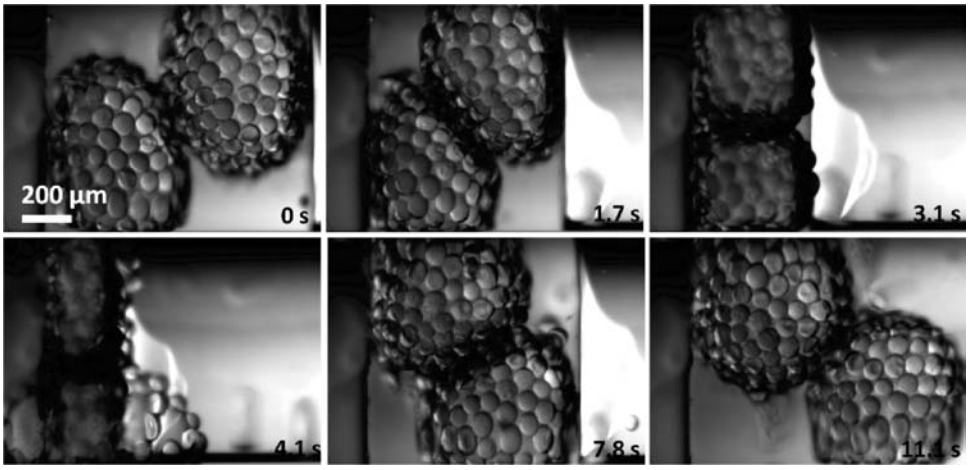

Figure 7. Series of still shot images showing the high stability of microparticle-coated silicone oil drops. Although two drops confined in a square capillary are squeezed together until 4.1 s, they do not coalesce because microparticle arrays at the interface prevent direct contact between the inner fluid interfaces.

Figure 9b−e. The convex surface shows hexagonal arrays of bare silica particles and sparsely distributed hydrophobic particles with low contact angle, as shown in Figure 9d. Although the concave surface has both types of silica particles, as shown in Figure 9e, we confirm that the bare silica particles are buried within the ETPTA matrix using higher-magnification SEM images.

Magneto-responsive amphiphilic microparticles can also be prepared through the addition of iron-oxide magnetic nanoparticles (α-Fe_2O_3, <50 nm) in the silica−ETPTA suspension before microfluidic emulsification. The resultant microparticles, with a brown color, can be concentrated by an external magnet, as shown in Figure S5 of Supporting Information.

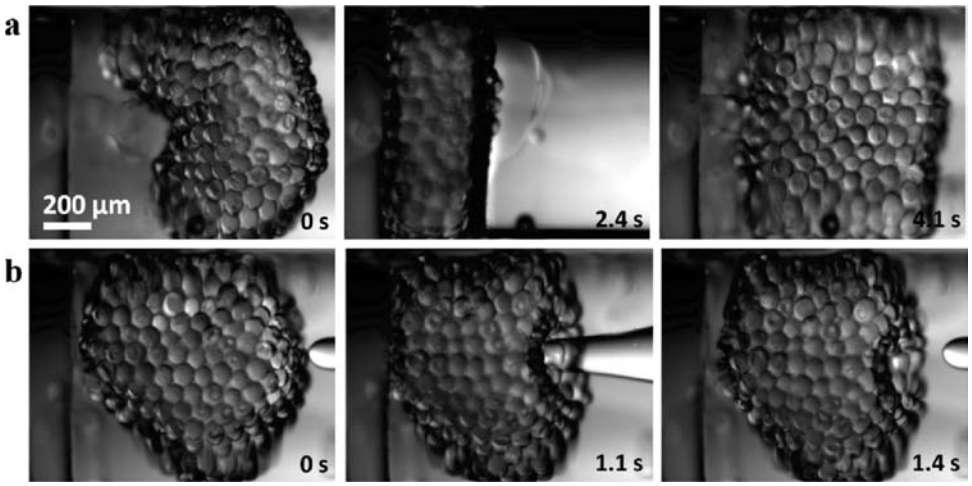

Figure 8. Series of still shot images showing immobilized interface of silicone oil drop by densely packed microparticles at the interface. (a) The nonspherical drop in a square capillary is squeezed by movable rods with flat ends, and the drop retains a square-disk shape after removal of the rod. (b) For pokes with glass cone, the interface is indented without puncture and maintains the dent even after removal of the cone.

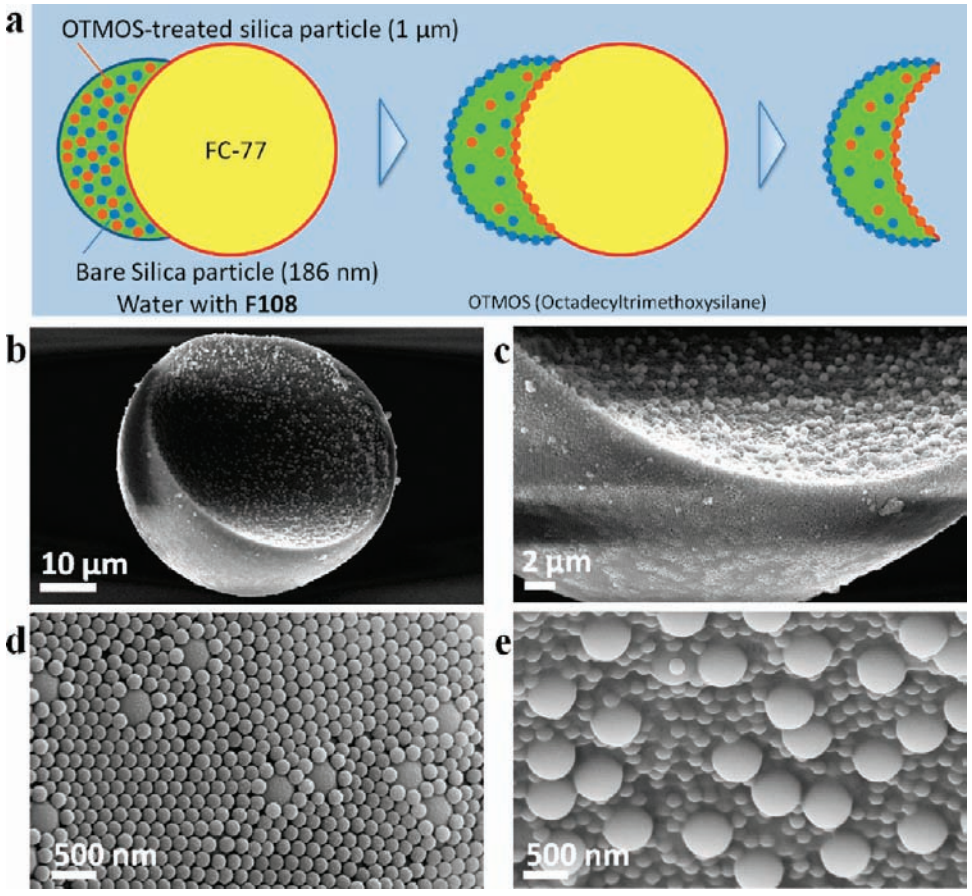

Figure 9. (a) Schematic illustration of the method to enhance contrast of wetting properties between convex and concave surfaces through a selective adsorption of two different silica particles. (b−e) SEM images of amphiphilic microparticles produced from the silica−ETPTA suspension containing bare hydrophilic silica (186 nm in diameter) and OTMOS (octadecyltrimethoxysilane)-treated hydrophobic silica particles (1 μm in diameter).

■ CONCLUSIONS

In this work, we report a facile microfluidic approach to create monodisperse amphiphilic microparticles with a crescent-moon shape, consisting of convex hydrophilic and concave hydrophobic surfaces. Using the amphiphilic character and the structural advantages of the crescent-moon shape, we stabilize and immobilize interfaces of oil drops with various sizes. Most previous nonspherical amphiliphilic microparticles were developed to stabilize drops of oil in water. To stabilize and functionalize the interfaces of inverted emulsions using amphiphilic particles

rather than molecular surfactants requires new classes of microparticles, and the crescent-moon-shaped particles presented here may represent a basis for further development to accomplish this. In addition, these amphiphilic microparticles have great potential for stabilization of gas−liquid interfaces, which is otherwise difficult to achieve with molecular surfactants.

■ ASSOCIATED CONTENT

Supporting Information. Optical microscope and SEM images of microparticles and particle-coated oil drops are included to show their structures and surface properties. This material is available free of charge via the Internet at http://pubs.acs.org.

Web Enhanced Feature. Movies S1−3 display details of droplet generation and response of particle-coated drops under mechanical disturbances. Movie S1 shows generation of droplets at the tip of the tapered theta-shaped capillary and the downstream motion of the paired droplets for F-108 surfactant and core-shell droplets for PVA surfactant. Movie S2 shows high stability of coated silicone oil drop with amphiphilic microparticles and immobilization of interface by densely packed microparticle array. Movie S3 shows comparison of mechanical responses of particle-coated silicone oil drop and PVA-stabilized oil drop by poking with glass cone rod.

■ AUTHOR INFORMATION

Corresponding Author
weitz@seas.harvard.edu

■ ACKNOWLEDGMENT

This work was supported by Amore-Pacific, the NSF (Grant DMR-1006546), and the Harvard MRSEC (Grant DMR-0820484).

■ REFERENCES

(1) Glotzer, S. C.; Solomon, M. J. *Nat. Mater.* **2007**, *6*, 557–562.
(2) Yang, S.-M.; Kim, S.-H.; Lim, J.-M.; Yi, G.-R. *J. Mater. Chem.* **2008**, *18*, 2177–2190.
(3) Nisisako, T.; Torii, T.; Takahashi, T.; Takizawa, Y. *Adv. Mater.* **2006**, *18*, 1152–1156.
(4) Kim, S.-H.; Jeon, S.-J.; Jeong, W.-C.; Park, H. S.; Yang, S.-M. *Adv. Mater.* **2008**, *20*, 4129–4134.
(5) Zhang, Z. L.; Keys, A. S.; Chen, T.; Glotzer, S. C. *Langmuir* **2005**, *21*, 11547–11551.
(6) Cho, Y.-S.; Yi, G.-R.; Lim, J.-M.; Kim, S.-H.; Manoharan, V. N.; Pine, D. J.; Yang, S.-M. *J. Am. Chem. Soc.* **2005**, *127*, 15968–15975.
(7) Binks, B. P.; Fletcher, P. D. I. *Langmuir* **2001**, *17*, 4708–4710.
(8) Perro, A.; Reculusa, S.; Ravaine, S.; Bourgeat-Lami, E.; Duguet, E. *J. Mater. Chem.* **2005**, *15*, 3745–3760.
(9) Hong, L.; Jiang, S.; Granick, S. *Langmuir* **2006**, *22*, 9495–9499.
(10) Hong, L.; Cacciuto, A.; Luijten, E.; Granick, S. *Nano Lett.* **2006**, *6*, 2510–2514.
(11) Kim, S.-H.; Lee, S. Y.; Yang, S.-M. *Angew. Chem., Int. Ed.* **2010**, *49*, 2535–2538.
(12) Kim, J.-W.; Larsen, R. J.; Weitz, D. A. *J. Am. Chem. Soc.* **2006**, *128*, 14374–14377.
(13) Kim, J.-W.; Lee, D.; Shum, H. C.; Weitz, D. A. *Adv. Mater.* **2008**, *20*, 3239–3243.
(14) Dendukuri, D.; Hatton, T. A.; Doyle, P. S. *Langmuir* **2007**, *23*, 4669–4674.
(15) Tanaka, T.; Okayama, M.; Minami, H.; Okubo, M. *Langmuir* **2010**, *26*, 11732–11736.
(16) Torza, S.; Mason, S. G. *J. Colloid Interface Sci.* **1970**, *33*, 67–83.
(17) Loxley, A.; Vincent, B. *J. Colloid Interface Sci.* **1998**, *208*, 49–62.
(18) Pannacci, N.; Bruus, H.; Bartolo, D.; Etchart, I.; Lockhart, T.; Hennequin, Y.; Willaime, H.; Tabeling, P. *Phys. Rev. Lett.* **2008**, *101*, No. 164502.
(19) Nisisako, T.; Torii, T. *Adv. Mater.* **2007**, *19*, 1489–1493.
(20) Nisisako, T.; Hatsuzawa, T. *Microfluid. Nanofluid.* **2010**, *9*, 427–437.
(21) Brakke, K. A. *Exp. Math.* **1992**, *1*, 141–165.
(22) Kim, S.-H.; Shim, J. W.; Lim, J. M.; Lee, S. Y.; Yang, S.-M. *New J. Phys.* **2009**, *11*, No. 075014.
(23) Binks, B. P.; Lumsdon, S. O. *Langmuir* **2000**, *16*, 8622–8631.
(24) Kim, S.-H.; Lee, S. Y.; Yi, G.-R.; Pine, D. J.; Yang, S.-M. *J. Am. Chem. Soc.* **2006**, *128*, 10897–10904.
(25) Huck, W. T. S.; Tien, J.; Whitesides, G. M. *J. Am. Chem. Soc.* **1998**, *120*, 8267–8268.
(26) Subramaniam, A. B.; Abkarian, M.; Mahadevan, L.; Stone, H. A. *Nature* **2005**, *438*, 930–930.
(27) Bausch, A. R.; Bowick, M. J.; Cacciuto, A.; Dinsmore, A. D.; Hsu, M. F.; Nelson, D. R.; Nikolaides, M. G.; Travesset, A.; Weitz, D. A. *Science* **2003**, *299*, 1716–1718.
(28) Abkarian, M; Subramaniam, A. B.; Kim, S.-H.; Larsen, R.; Yang, S.-M.; Stone, H. A. *Phys. Rev. Lett.* **2007**, *99*, No. 188301.